neously oscillating about the equatorial plane by $a[\sin(i)]$. All three excursions—radial, longitudinal, and vertical—occur nearly at the orbital frequency.
23. D. P. Hamilton, *Icarus* **101**, 244 (1993).
24. M. Horanyi, *Annu. Rev. Astron. Astrophys.* **34**, 383 (1996).
25. J. A. Burns *et al.*, *Nature* **316**, 115 (1985).
26. D. P. Hamilton, *Icarus* **109**, 221 (1994); L. Schaffer and J. A. Burns, *ibid.* **96**, 65 (1992).
27. J. A. Burns, J. N. Cuzzi, M. R. Showalter, *Bull. Am. Astron. Soc.* **15**, 1013 (1983); M. R. Showalter, J. A. Burns, D. P. Hamilton, *ibid.* **30**, 1044 (1998); C. D. Murray, M. K. Gordon, S. M. Giuliatti-Winter, *Icarus* **129**, 304 (1997).
28. This research was supported by grants from NASA as well as by the Galileo Project. We acknowledge the help of the Galileo imaging team, especially M. J. S. Belton, J. Veverka, T. V. Johnson, K. Klaasen, and H. Breneman, in obtaining these data.

14 January 1999; accepted 9 April 1999

65,000 Years of Vegetation Change in Central Australia and the Australian Summer Monsoon

B. J. Johnson,[1,2*†] G. H. Miller,[2] M. L. Fogel,[1] J. W. Magee,[3] M. K. Gagan,[4] A. R. Chivas[5]

Carbon isotopes in fossil emu (*Dromaius novaehollandiae*) eggshell from Lake Eyre, South Australia, demonstrate that the relative abundance of C_4 grasses varied substantially during the past 65,000 years. Currently, C_4 grasses are more abundant in regions that are increasingly affected by warm-season precipitation. Thus, an expansion of C_4 grasses likely reflects an increase in the relative effectiveness of the Australian summer monsoon, which controls summer precipitation over Lake Eyre. The data imply that the Australian monsoon was most effective between 45,000 and 65,000 years ago, least effective during the Last Glacial Maximum, and moderately effective during the Holocene.

The Lake Eyre Basin (LEB) extends across one-sixth of Australia's arid and semiarid zones (Fig. 1). Data from lacustrine, fluvial, and eolian deposits within the LEB show that the climate varied during the Quaternary (*1, 2*). These changes exerted a dominant control on vegetation; however, paleovegetation records in the Australian interior are sparse, particularly before 18,000 years ago (18 ka) (*3, 4*). Long-term paleovegetation records for central Australia are important for understanding the interplay between natural climate variability, the arrival of the first human immigrants [~60 ka (*5*)], and the extinction of an element of the Australian megafauna, *Genyornis newtoni* [~50 ka (*6*)]. In our study, we used stable carbon isotopes in emu eggshell (EES) calcite from Lake Eyre, South Australia, to develop a proxy for paleovegetation over the past 65,000 years.

The carbon isotope composition ($\delta^{13}C$) (*7*) of avian eggshell reflects the isotopic composition of the bird's diet integrated over 3 to 5 days (*8*), offset by a biochemical fractionation (*9*). EES carbonate is enriched in ^{13}C by 10 ± 2 per mil relative to the diet (Web Table 1, available at www.sciencemag.org/feature/data/990227.shl). During the egg-laying season [July through September (*10*)], emus are primarily mixed-feeder herbivores, consuming leaves, shoots, fruits, and flowers of trees, shrubs, forbs, and grasses (*11*). Variations in the $\delta^{13}C$ values of EES ($\delta^{13}C_{EES}$) reflect changes in emu diet, which are ultimately driven by changes in the isotopic composition of the flora.

Two isotopically distinct sets of plants dominate the Australian interior: those with C_3 (average $\delta^{13}C$ = –26.5 per mil) or those with C_4 (average $\delta^{13}C$ = –12.5 per mil) photosynthetic pathways (*12–14*). In Australia, the photosynthetic pathway of grasses depends primarily on the most effective season of rainfall and varies from north to south (*12*). C_3 grasses dominate in regions most affected by winter precipitation (southern Australia), and C_4 grasses become increasingly dominant in regions increasingly affected by summer monsoonal precipitation (central to northern Australia). Almost all of the trees, shrubs, and forbs across Australia are C_3 plants.

We hypothesize that $\delta^{13}C_{EES}$ from Lake Eyre reflects changes in the relative proportion of C_3 to C_4 vegetation and therefore serves as an indirect proxy for the predominant season of rainfall during the past 65 ka. To test this hypothesis, we measured $\delta^{13}C$ in the carbonate fraction of 55 modern EESs from a range of seasonal precipitation and vegetation regimes across Australia (Fig. 1 and Web Table 1). We then compared the $\delta^{13}C$ of modern EES and ambient vegetation with the $\delta^{13}C$ of 219 dated (*15*) fossil EESs from deposits located along the southeastern border of Lake Eyre (Web Table 2, available at www.sciencemag.org/feature/data/990227.shl) (*16*).

The $\delta^{13}C$ values of modern EES mirror the photosynthetic pathways that prevail locally; a pure C_3 signal is found in the south, where all plants (including grasses) use the C_3 pathway, and a mixed C_3-C_4 signal is found in the north as a result of the inclusion

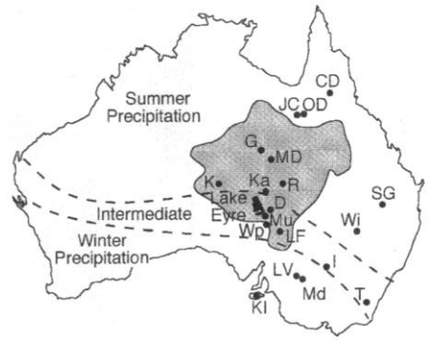

Fig. 1. Map of the Australian mainland and Kangaroo Island (KI), illustrating the locations (solid circles) of sampling sites of modern EES, Lake Eyre, and the Lake Eyre Basin (gray region). Site locations are abbreviated as follows: CD, Carpentaria Downs, QLD; JC, Millungera, QLD; OD, Olga Downs, QLD; G, Glenormiston, QLD; MD, Marion Downs, QLD; K, Kulgera, NT; Ka, Kallakoopah Creek, SA; R, Roseberth, QLD; D, Dulkanina, SA; SG, St. George, QLD; Mu, Muloorina, SA; Wi, Wirrona, NSW; Wp, Wilpoorinna, SA; LF, Lake Froma, SA; I, Ivanhoe, NSW; LV, Lake Victoria, NSW; Md, Mildura, NSW; and T, Tidbinbilla, NSW. Precipitation across northern and central Australia is highly seasonal; the Australian monsoon delivers precipitation to the north during the summer months, and the westerly storm track delivers precipitation to the south during the winter months (*30*). Dashed lines represent the approximate boundaries between the areas influenced primarily by the Australian monsoon and the westerly storm tracks. The intermediate area receives a modicum of precipitation throughout the year.

[1]Geophysical Laboratory, Carnegie Institution of Washington, 5251 Broad Branch Road, NW, Washington, DC 20015–1305, USA. [2]Institute of Arctic and Alpine Research and Department of Geological Sciences, University of Colorado, Boulder, CO 80309–0450, USA. [3]Department of Geology, [4]Research School of Earth Sciences, Australian National University, Canberra ACT 0200, Australia. [5]School of Geosciences, University of Wollongong, Wollongong NSW 2522, Australia.

*Present address: School of Oceanography, University of Washington, Seattle, WA 98195–7940, USA.
†To whom correspondence should be addressed. E-mail: bjohnson@ocean.washington.edu

of C_4 grasses in emu diets (Fig. 2). The $\delta^{13}C_{EES}$ values reflect an overall increase in C_4 grass consumption in areas increasingly influenced by the summer monsoon. Emu eggs are laid during the winter months; thus, a dietary preference for C_3 plants, which often flower and seed in winter (*17*), and a dietary bias against seasonally burned or senescent summer C_4 grasses is probably reflected in the $\delta^{13}C$ values. Nevertheless, EES collected from C_4 grasslands near Julia Creek indicate that emus can subsist on up to 70% C_4 grasses during the egg-laying season. Our modern calibration data set confirms that the $\delta^{13}C$ of modern EES reflects that of ambient vegetation and serves as an indirect proxy for the effectiveness of the summer monsoon.

Between 65 and 45 ka, $\delta^{13}C_{EES}$ values are highly variable [average $\delta^{13}C$ value ($\delta^{13}C_{avg}$) = −6.4 ± 4.0 per mil; n = 85], with a significant proportion of the population subsisting either entirely on C_4 plants or on C_3 plants (Fig. 3). The bimodal distribution of the isotopic data may result from relatively short-lived climatic oscillations during this time interval—periods when the summer monsoon was highly effective and C_4 grasses dominated and vice versa. These climatic oscillations would have occurred over periods shorter than the resolution of current dating techniques [±8000 years for samples older than 40 ka (*6, 15*)]. Alternatively, the ecosystem may have been stable and dominated by C_4 grasses, with some C_3 shrubs and trees, similar to the savanna grasslands of Africa. These isotopic data imply that the Australian summer monsoon was highly effective during much of this time interval or that its intensity varied greatly.

Between 28 and 15 ka, the $\delta^{13}C_{EES}$ values decrease and are less variable ($\delta^{13}C_{avg}$ = −11.8 ± 1.3 per mil; n = 23), reflecting a near total absence of C_4 grasses during the Last Glacial Maximum (LGM). This contrasts with paleovegetation records from tropical Africa (*18*) and the southwestern United States (*19*), where expansion of C_4 grasslands occurs. During the LGM, atmospheric pressure of CO_2 (PCO_2) values were ~190 parts per million by volume (*20*), and the average mean annual temperature at Lake Eyre was ~11°C (*21*), conditions favoring the crossover from C_3 to C_4 grasslands (*22*). On the basis of the $\delta^{13}C_{EES}$ values, we surmise that the low temperatures and reduced warm-season precipitation of the LGM overwhelmed any PCO_2-induced shift toward increased C_4 grass biomass at Lake Eyre.

The $\delta^{13}C$ values of Holocene EES are slightly higher ($\delta^{13}C_{avg}$ = −9.9 ± 1.6 per mil; n = 43) than the LGM EES, suggesting that the range of C_4 plants expanded, although in much lower proportions than the range before 45 ka. Decreased global aridity at the end of the last glaciation and a decrease in chenopod/grass ratios at nearby Lake Frome (*4*) support our interpretation that the isotopic change observed at the LGM-Holocene transition results from the expansion of C_4 grasses at Lake Eyre and, at least, irregular increases in monsoonal moisture. Thus, the Holocene Australian summer monsoon was more effective than the LGM monsoon but much less effective than the monsoon between 65 and 45 ka.

A major isotopic shift has been measured in samples postdating European colonization of the LEB (~150 years ago) ($\delta^{13}C_{avg}$ = −12.5 ± 1.3 per mil; n = 9) in relation to EES dated between 2 and 1 ka ($\delta^{13}C_{2\text{-}1ka}$ = −8.9 ± 2.1 per mil; n = 7). Less than half of the 4 per mil isotopic depletion in modern EES may be explained by the decrease of 1.5 per mil in isotopic composition of atmospheric CO_2 concomitant with the industrial revolution (*23*). We surmise that the remaining isotopic depletion of 2.5 per mil in modern samples results from the arrival of European pastoralists and the introduction of exotic animals. Overgrazing or trampling of grasses [which are primarily C_4 at Lake Eyre (*12*)] by nonnative animals (sheep and rabbits), changes in fire regimes, and extinction of smaller marsupials should bias the ecosystem toward C_3 vegetation (*24*). These data suggest that grassland ecosystems declined greatly across the semiarid zone of Australia, without obvious changes in monsoonal forcing.

Over the past 65,000 years, environmental factors other than climate have substantially influenced Australian ecology (*25*). Vegetation change in northeastern and southeastern Australia, brought about by an increase in fire frequency (*26*), has been attributed to the arrival of the first human immigrants at ~60 ka (*5*) and has been suggested as the cause of extinction of *G. newtoni* at ~50 ka (*6*). Our isotopic data are consistent with a human overprint on natural climate change. The effectiveness of the summer monsoon at Lake Eyre decreased substantially at approximately the same time as megafauna extinction (*6*) and never fully recovered, despite an invigorated planetary monsoon during the early Holocene (*27*). The transfer of moisture from the biosphere to the atmosphere is an important feedback mechanism that enhances the penetration of monsoon moisture into the interior of other continents (*28*). A change in vegetation type across northern Australia brought about by the burning practices of the first human colonizers may have reduced this wet-season feedback and, consequently, diminished the effectiveness of the summer monsoon at Lake Eyre during the early Holocene (*29*). Continuous records of vegetation change from the semiarid interior of central and northern Australia, such as the one presented here, are required to evaluate the magnitude of human impact.

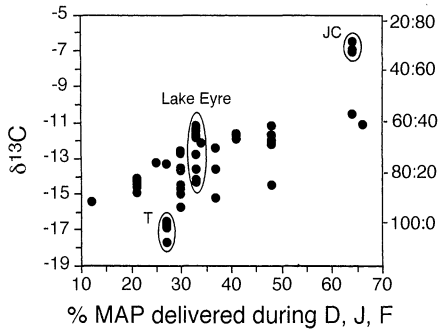

Fig. 2. The $\delta^{13}C$ of modern EES calcite versus the percentage of mean annual precipitation (% MAP) delivered to the collection site during the summer months [December, January, and February (D, J, F)] (*31*) and the ratio of C_3:C_4 plants consumed, calculated from the $\delta^{13}C_{EES}$ values (*32*). The three collection sites circled illustrate the variability expected within individual nests [$\delta^{13}C_{avg}$ at JC = −6.8 ± 0.3 per mil (n = 3) and $\delta^{13}C_{avg}$ at T = −16.8 ± 0.4 per mil (n = 8)] and variability expected for specific precipitation regimes [$\delta^{13}C_{avg}$ at Lake Eyre (Mu, D, and Wp) = −12.5 ± 1.3 per mil (n = 9)]. The isotopic variability measured within specific precipitation regimes results from changes in feeding patterns during the egg-laying season and a response to interannual differences in rainfall with consequent impacts on vegetation over the 17-year sampling interval. In the fossil record, neither of these factors can be controlled; thus, detection of long-term trends requires analysis of large suites of eggshells (>10) from each time period.

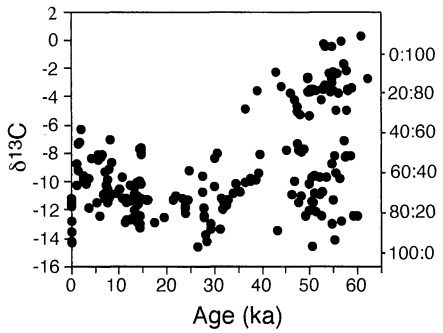

Fig. 3. The $\delta^{13}C$ of fossil EES calcite from sites across the southern margin of Lake Eyre versus sample age (calibrated to calendar years) and the ratio of C_3:C_4 plants consumed, as estimated from the $\delta^{13}C_{EES}$. Dietary calculations have been adjusted for preindustrial atmospheric CO_2 $\delta^{13}C$ values by assuming that the average $\delta^{13}C$ values of preindustrial C_3 and C_4 plants were 1.5 per mil more enriched in ^{13}C than present values. The data are discussed in four different blocks of time, which are defined on the basis of consistency in the isotopic data as follows: 65 to 45 ka (largest range and most isotopically enriched values), 28 to 15 ka (isotopically depleted values), 10 to 1 ka (moderate isotopic values), and samples younger than 150 years old (isotopically depleted values).

References and Notes

1. G. C. Nanson, D. M. Price, S. A. Short, *Geology* **20**, 791 (1992); J. Croke, J. Magee, D. Price, *Palaeogeogr. Palaeoclimatol. Palaeoecol.* **124**, 1 (1996); J. M. Bowler and R. J. Wasson, in *Late Cainozoic Paleoclimates of the Southern Hemisphere*, J. C. Vogel, Ed. (Balkema, Rotterdam, 1984), pp. 183–208; J. M. Bowler, in *Evolution of the Flora and Fauna of Arid Australia*, W. R. Barker and P. J. M. Greenslade, Eds. (Peacock Publications, Frewville, SA, Australia, 1982), pp. 35–45; R. J. Wasson, *Geogr. Rev. Jpn. Ser. B* **59**, 55 (1986).
2. J. W. Magee, J. M. Bowler, G. H. Miller, D. L. G. Williams, *Palaeogeogr. Palaeoclimatol. Palaeoecol.* **113**, 3 (1995); J. W. Magee, thesis, Australian National University, Canberra (1997); _____ and G. H. Miller, *Palaeogeogr. Palaeoclimatol. Palaeoecol.* **144**, 307 (1998).
3. S. Pearson and J. R. Dodson, *Quat. Res.* **39**, 347 (1993); L. McCarthy, L. Head, J. Quade, *Palaeogeogr. Palaeoclimatol. Palaeoecol.* **123**, 205 (1996); J. G. Luly, *J. Biogeogr.* **20**, 587 (1993).
4. G. Singh and J. Luly, *Palaeogeogr. Palaeoclimatol. Palaeoecol.* **84**, 75 (1991).
5. R. G. Roberts, R. Jones, M. A. Smith, *Nature* **345**, 153 (1990); R. G. Roberts *et al.*, *Quat. Sci. Rev.* **13**, 575 (1994).
6. G. H. Miller *et al.*, *Science* **283**, 205 (1999).
7. Isotopic data are reported in δ values, where $\delta^{13}C$ (in per mil) = $[(^{13}C/^{12}C)_{sample}/(^{13}C/^{12}C)_{standard} - 1] \times 1000$, and the isotopic standard is Vienna Pee Dee belemnite, calibrated through National Bureau of Standards reference materials.
8. K. A. Hobson, *Condor* **97**, 752 (1995).
9. Y. von Schirnding, N. J. Van der Merwe, J. C. Vogel, *Archaeometry* **24**, 3 (1982); B. J. Johnson, M. L. Fogel, G. H. Miller, *Geochim. Cosmochim. Acta* **62**, 2451 (1998).
10. C. L. Coddington, thesis, Australian National University, Canberra (1992).
11. S. J. J. F. Davies, *Aust. J. Ecol.* **3**, 411 (1978); T. J. Dawson, D. Read, E. M. Russell, R. M. Herd, *Emu* **84**, 93 (1984).
12. P. W. Hattersley, *Oecologia* **57**, 113 (1983).
13. N. Nicholls, *Vegetatio* **91**, 23 (1991).
14. B. N. Smith and S. Epstein, *Plant Physiol.* **47**, 380 (1971).
15. The fossil eggshells were dated by direct accelerator mass spectrometry (AMS) ^{14}C (n = 77) and from the extent of amino acid racemization [D-alloisoleucine/L-isoleucine (D/L); n = 219]. For those samples not directly dated by AMS ^{14}C, we used the age model of Miller *et al.* (*6*) to assign ages to each D/L value. Errors in converting D/L to age are primarily related to the depth of burial and the low rate of racemization during the cold interval between 15 and 40 ka (*21*). Comparing ^{14}C-D/L model-age pairs between 0 and 14.5 ka, we found that the average error is 1600 years. For the period between 14.5 and 36 ka, ^{14}C-D/L model age pairs have an average error of 7900 years because temperatures were low and most LGM deposits are <2 m thick. We cannot formally evaluate the error for older samples, but because the deposits are much thicker (>4 m) and temperatures were warmer, the model-age error should be less.
16. For isotopic analyses of the EES calcite, between 2 and 3 mg of ground EES were reacted with 100% H_3PO_4 at 60°C, and the resultant CO_2 was analyzed with a Finnigan MAT 252 mass spectrometer (Geophysical Laboratory), or between 100 and 150 mg of ground EES were reacted with 105% H_3PO_4 at 90°C with an automated individual carbonate reaction Kiel device coupled with a Finnigan MAT 251 mass spectrometer (Research School of Earth Sciences). The carbon isotopic offset between the inorganic and total organic fractions of EES (as defined by $\Delta^{13}C = \delta^{13}C_{inorg} - \delta^{13}C_{org}$) was used as a means to evaluate the amount of isotopic exchange that occurred in the fossil samples. The average $\Delta^{13}C$ of modern EES was 9.0 ± 1.0 per mil (n = 37), regardless of the $\delta^{13}C$ value of the diet (Web Table 1), and the average $\Delta^{13}C$ of fossil EES was 10.4 ± 2.0 per mil (n = 45) (Web Table 2). The general agreement between the $\Delta^{13}C$ values of modern and fossil EES implies excellent preservation of both eggshell fractions through geologic time; however, seven EESs with $\Delta^{13}C$ values greater than $\pm 2\sigma$ from the average modern $\Delta^{13}C$ value were excluded from the data analysis (Web Table 2).
17. P. Latz, *Bushfires and Bushtucker* (Institute for Aboriginal Development Press, Alice Springs, NT, Australia, 1995).
18. A.-M. Aucour *et al.*, *Quat. Res.* **41**, 224 (1994); F. A. Street-Perrott *et al.*, *Science* **278**, 1422 (1997).
19. B. Liu, F. M. Phillips, A. R. Cambell, *Palaeogeogr. Palaeoclimatol. Palaeoecol.* **124**, 233 (1996); S. L. Connin, J. Betancourt, J. Quade, *Quat. Res.* **50**, 179 (1998).
20. J. M. Barnola, D. Raynaud, Y. S. Korotkevich, C. Lorius, *Nature* **329**, 408 (1987).
21. G. H. Miller, J. W. Magee, A. J. T. Jull, *ibid.* **385**, 241 (1997).
22. T. E. Cerling *et al.*, *ibid.* **389**, 153 (1997).
23. B. D. Marino and M. B. McElroy, *ibid.* **349**, 127 (1991).
24. J. C. Noble, *The Delicate and Noxious Scrub* (Commonwealth Scientific and Industrial Research Organisation, Canberra, 1997); D. A. Adamson and M. D. Fox, in *A History of Australian Vegetation*, J. M. B. Smith, Ed. (McGraw-Hill, Sydney, 1982), pp. 109–146.
25. T. Flannery, *The Future Eaters* (Reed Books, Melbourne, 1994).
26. A. P. Kershaw, *Nature* **322**, 47 (1986); G. Singh and E. A. Geissler, *Philos. Trans. R. Soc. London Ser. B* **311**, 379 (1985).
27. W. L. Prell and J. E. Kutzbach, *J. Geophys. Res.* **92**, 8411 (1987); Z. An, G. J. Kukla, S. C. Porter, J. Xiao, *Quat. Res.* **36**, 29 (1991); J. L. Xiao *et al.*, *Quat. Sci. Rev.* **18**, 147 (1999).
28. A. Henderson-Sellers *et al.*, *J. Geophys. Res.* **98**, 7289 (1993); J. Kutzbach, G. Bonan, J. Foley, S. P. Harrison, *Nature* **384**, 623 (1996).
29. G. H. Miller and J. W. Magee, *Eos Trans. Am. Geophys. Union Fall Meet. Suppl.* **73** (no. 43), 104 (1992).
30. N. J. Tapper and L. Hurry, *Australia's Weather Patterns: An Introductory Guide* (Dellasta, Mount Waverley, VIC, Australia, 1993); J. Gentilli, Ed., in *Climates of Australia and New Zealand*, (Elsevier, Amsterdam, 1971), pp. 53–117.
31. Mean monthly precipitation values at meteorological stations closest to the eggshell collection sites were provided by the Commonwealth Bureau of Meteorology, Melbourne (available at www.bom.gov.au/climate/averages).
32. The ratio of C_3 to C_4 plants in emu diets was calculated from $\delta^{13}C_{EES}$ values using a two–end-member mixing model as follows:

$$\delta^{13}C_{EES} - BF = \delta^{13}C_{C3}(X) + \delta^{13}C_{C4}(1 - X),$$

where BF is biochemical fractionation (10 per mil for EES calcite), $\delta^{13}C_{C3} = -26.5$ per mil, $\delta^{13}C_{C4} = -12.5$ per mil, and X is the proportion of C_3 plants in the diet. The variability associated with the BF and the isotopic compositions of the end-members corresponds to an uncertainty of ±15% in the C_3:C_4 dietary calculations; thus, these calculations are primarily useful for comparative purposes.

33. This research was funded by the International Programs Division (B.J.J.) and the Division of Atmospheric Science of NSF (B.J.J., G.H.M., and M.L.F.), the Geophysical Laboratory at the Carnegie Institution of Washington, and the Australian National University. We thank G. Atkin, S. Webb, O. Miller, and P. Clark for assistance in obtaining samples; C. Hart and J. Cali for laboratory assistance; and P. Koch, J. Luly, M. Duvall, K. Hughen, M. Teece, V. Sloan, and J. Brandes for comments on early drafts of the manuscript.

14 January 1999; accepted 9 April 1999

Electrostatic Modulation of Superconductivity in Ultrathin $GdBa_2Cu_3O_{7-x}$ Films

C. H. Ahn, S. Gariglio, P. Paruch, T. Tybell, L. Antognazza, J.-M. Triscone

The polarization field of the ferroelectric oxide lead zirconate titanate [$Pb(Zr_xTi_{1-x})O_3$] was used to tune the critical temperature of the high-temperature superconducting cuprate gadolinium barium copper oxide ($GdBa_2Cu_3O_{7-x}$) in a reversible, nonvolatile fashion. For slightly underdoped samples, a uniform shift of several Kelvin in the critical temperature was observed, whereas for more underdoped samples, an insulating state was induced. This transition from superconducting to insulating behavior does not involve chemical or crystalline modification of the material.

Superconductor-insulator transitions have been investigated theoretically and experimentally in a variety of systems, including three-dimensional (3D) ionic crystals, 2D films, and Josephson junction arrays. These transitions are examples of the modulation of superconductivity by means of control parameters such as pressure, magnetic field, disorder, and thickness (*1–4*). For applications, superconducting bolometers operate on changes in the temperature, and superconducting quantum interference devices rely on the application of small magnetic fields that modulate the critical current of a Josephson junction.

Here we report on nonvolatile, reversible modulation of superconductivity in the high-temperature copper oxide superconductor $GdBa_2Cu_3O_{7-x}$ (GBCO), using an electrostatic field as the control parameter. A unique feature of these cuprate materials, as compared to the elemental BCS superconductors, is that their properties depend strongly on the carrier concentration, as shown by their generic temperature-doping phase diagram (Fig. 1), which depicts an antiferromagnetic insulating state at low doping levels that is

Département de Physique de la Matière Condensée, University of Geneva, 24 Quai Ernest-Ansermet, 1211 Geneva 4, Switzerland.